

Oscillatory instability of traveling waves for a KdV–Burgers equation

Robert L. Pego,^{a,1} Peter Smereka,^{b,2} and Michael I. Weinstein^{c,3}

^aDepartment of Mathematics and Institute for Physical Science and Technology, University of Maryland, USA

^bDepartment of Mathematics, University of California at Los Angeles, USA

^cDepartment of Mathematics, University of Michigan, Ann Arbor, USA

Received 12 August 1992

Revised manuscript received 21 January 1993

Accepted 26 February 1993

Communicated by H. Flaschka

The stability of traveling wave solutions of a generalization of the KdV–Burgers equation: $\partial_t u + u^p \partial_x u + \partial_x^3 u = \alpha \partial_x^2 u$, is studied as the parameters p and α are varied. The eigenvalue problem for the linearized evolution of perturbations is analyzed by numerically computing Evans' function, $D(\lambda)$, an analytic function whose zeros correspond to discrete eigenvalues. In particular, the number of unstable eigenvalues in the complex plane is evaluated by computing the winding number of $D(\lambda)$. Analytical and numerical evidence suggests that a Hopf bifurcation occurs for oscillatory traveling wave profiles in certain parameter ranges. Dynamic simulations suggest that the bifurcation is *subcritical* – no stable time periodic solution is found.

1. Introduction

We consider the generalized KdV–Burgers equation

$$\partial_t u + u^p \partial_x u + \partial_x^3 u = \alpha \partial_x^2 u, \quad (1.1)$$

a model for long wave propagation in nonlinear media with dispersion and dissipation. Here $p \geq 1$ and $\alpha > 0$. The case $p = 1$ is known as the KdV–Burgers equation; it has been derived as an equation which describes the propagation of undular bores in shallow water [3,15], and weakly nonlinear plasma waves with certain dissipative effects [11,13,17].

For $\alpha = 0$, eq. (1.1), now a generalized KdV equation (gKdV), has solitary wave solutions $u(x, t) = \phi_0(x - ct)$ for any $c > 0$, whose profile $\phi_0(\xi)$ satisfies

$$-c\phi_0 + \frac{1}{p+1} \phi_0^{p+1} + \partial_\xi^2 \phi_0 = 0, \quad \phi_0(\xi) \rightarrow 0 \quad \text{as } \xi \rightarrow \pm\infty. \quad (1.2)$$

Explicitly,

$$\phi_0(\xi) = \beta \operatorname{sech}^{2/p} \gamma \xi, \quad \beta = [\tfrac{1}{2}c(p+1)(p+2)]^{1/p}, \quad \gamma = \tfrac{1}{2}p\sqrt{c}.$$

¹ Supported by NSF Grant DMS DMS-9201869.

² Supported by a National Science Foundation Postdoctoral Fellowship.

³ Supported by NSF Grant DMS-9201717.

This wave is known to undergo a transition from stability ($p < 4$) to instability ($p > 4$) as the parameter p passes through the critical value $p_{cr} = 4$, cf. [2,4,6,19,24,29–31].

For $\alpha > 0$, eq. (1.1) has a family of traveling wave solutions, whose properties are summarized as follows (cf. [5,24]).

Theorem 1.1. Given $\alpha > 0$ and $c > 0$, eq. (1.1) has a solution $u(x, t) = \phi(x - ct)$, unique up to translation, with wave profile $\phi(\xi)$ satisfying

$$-c\phi + \frac{1}{p+1} \phi^{p+1} + \partial_\xi^2 \phi = \alpha \partial_\xi \phi, \quad \xi \in \mathbb{R}, \tag{1.3}$$

$$\phi(\xi) \rightarrow \begin{cases} u_L & \text{as } \xi \rightarrow -\infty, \\ 0 & \text{as } \xi \rightarrow \infty. \end{cases} \tag{1.4}$$

Here, $u_L = [c(p+1)]^{1/p}$ is the unique positive solution of $-cu_L + u_L^{p+1}/(p+1) = 0$. If $\alpha > 2\sqrt{pc}$, the profile ϕ is monotonically decreasing, while if $\alpha < 2\sqrt{pc}$, then $\phi(\xi) \rightarrow u_L$ in an oscillatory fashion as $\xi \rightarrow -\infty$. As $\xi \rightarrow +\infty$, the profile satisfies

$$\phi(\xi) \sim e^{\nu(\xi - \xi_0)}, \quad \partial_\xi \phi(\xi) \sim \nu e^{\nu(\xi - \xi_0)}, \tag{1.5}$$

for some ξ_0 , where $\nu = \frac{1}{2}(\alpha - \sqrt{\alpha^2 + 4c}) < 0$.

In the $\phi - \phi'$ phase plane, the wave profile corresponds to the unique trajectory that connects the unstable critical point $(u_L, 0)$ to the saddle point $(0, 0)$. See fig. 1.

As $\alpha \rightarrow 0$ for fixed c, p (and ξ_0), the wave profile converges in a very nonuniform fashion. At $\alpha = 0$, the stable manifold of the saddle point $(0, 0)$ is a *homoclinic loop* given by the level curve $E = 0$ of the conserved quantity

$$E(\phi, \phi') = \frac{1}{2} \phi'^2 - \frac{1}{2} c \phi^2 + \frac{1}{(p+1)(p+2)} \phi^{p+2}. \tag{1.6}$$

Level curves for $E < 0$ correspond to closed periodic orbits lying inside the homoclinic loop and encircling a center at $(u_L, 0)$. As α becomes positive, the homoclinic loop breaks, and because

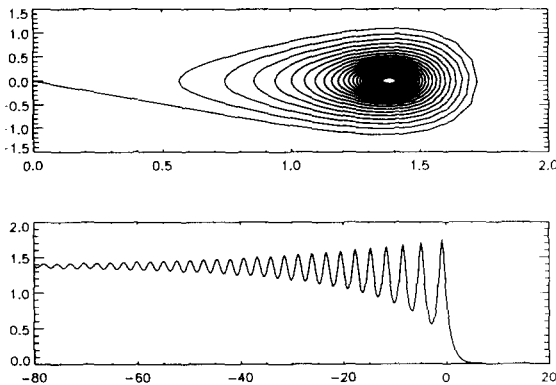


Fig. 1. Top: $\phi - \phi'$ phase plane. Bottom: $\phi(\xi)$ versus ξ .

$dE/d\xi = \alpha\phi'^2 \geq 0$, the stable manifold is trapped in the region $E < 0$, approaching the unstable spiral point $(u_L, 0)$ as $\xi \rightarrow -\infty$; it fills the region $E < 0$ ever more densely as $\alpha \rightarrow 0$. Assuming ξ_0 is fixed in (1.5), as $\alpha \rightarrow 0$ the wave profile $\phi(\xi)$ converges uniformly on any *half line* $\xi \geq x_0$ (x_0 fixed) to the solitary wave profile $\phi_0(\xi)$ of the gKdV equation. But $\phi(\xi)$ and $\phi_0(\xi)$ behave very differently in the limit $\xi \rightarrow -\infty$. On the one hand $\phi_0(\xi) \rightarrow 0$, while for small $\alpha > 0$, $\phi(\xi) \rightarrow u_L \neq 0$ in an oscillatory fashion.

Now, when $\alpha > 2\sqrt{pc}$, the wave profile $\phi(\xi)$ is monotone, and the traveling wave $\phi(x - ct)$ is known to be stable [23,24]. When $\alpha - 2\sqrt{pc}$ is negative but sufficiently small, the wave profile is “mildly oscillatory” and stability persists [18]. No rigorous results establishing stability or instability are available for highly oscillatory waves corresponding to small values of $\alpha > 0$. But numerical experiments of Canosa and Gazdag [7] suggest that for the KdV–Burgers equation (the case $p = 1$), these waves may be stable.

In the case $p > 4$, however, it is reasonable to conjecture that a transition to instability occurs as α decreases to zero. The rightmost ‘hump’ of the wave profile converges in shape to the profile of the unstable solitary wave $\phi_0(x - ct)$ which exists for $\alpha = 0$. In fact, it is known [24] that for $p > 4$ and $\alpha = 0$, the linearized evolution equation, governing perturbations of this solitary wave, admits a solution of the form $e^{\lambda_0 t} Y(x)$ where $\lambda_0 > 0$ is an eigenvalue of the linearized operator A_0 (described in section 2). As p passes through the critical value $p_{cr} = 4$, the eigenvalue $\lambda_0 = \lambda_0(p)$ emerges from the origin: we have $\lambda_0(p) \rightarrow 0$ as $p \rightarrow 4$ from above.

Since $\phi_0(x - ct)$ is unstable for $p > 4$, this suggests that the wave $\phi(x - ct)$ should be unstable for small $\alpha > 0$. But a rigorous result is not immediately available – the radically different behavior of the wave profiles $\phi(\xi)$ and $\phi_0(\xi)$ in the limit $\xi \rightarrow -\infty$ makes it difficult to relate the eigenvalue problem for one to that for the other.

Indeed, some results proved in [24] show that if the wave $\phi(x - ct)$ does become unstable as $\alpha \rightarrow 0$, then the mechanism by which this would occur must differ from that by which the solitary wave $\phi_0(x - ct)$ becomes unstable as p passes through $p_{cr} = 4$. In particular, from [24] it follows that, for the linearized evolution equation for perturbations of the wave $\phi(x - ct)$, no eigenvalue $\lambda_0(\alpha)$ can emerge from the origin as long as $\alpha > 0$. (See the discussion in section 3 below.)

This result suggests that if the wave $\phi(x - ct)$ is in fact linearly exponentially unstable for small $\alpha > 0$ when $p > 4$, the transition to instability would involve complex eigenvalues crossing the imaginary axis. This in turn suggests that a Hopf bifurcation may occur, and time-periodic solutions of (1.1) may exist.

In the present paper, we present numerical evidence that the wave $\phi(x - ct)$ is indeed linearly exponentially unstable for small $\alpha > 0$ when $p > 4$, and that transition to instability does involve a single pair of complex eigenvalues crossing the imaginary axis transversally as α decreases. Actually, we prove that if instability occurs, then there is a critical value of α at which a pair of nonzero purely imaginary complex conjugate eigenvalues exists. See theorem 3.5. We consider it likely that a Hopf bifurcation does occur, but the issue is clouded by the fact that the linearization admits a zero eigenvalue, and essential spectrum that contains the origin.

We also present numerical experiments which suggest that as α is decreased, the wave $\phi(x - ct)$ loses stability via a *subcritical* Hopf bifurcation [21] – no stable time periodic solutions are found. Instead, dynamic simulations are consistent with a scenario in which unstable time-periodic solutions exist.

Lastly, as α is decreased further, we numerically observe additional pairs of complex eigenvalues cross into the right half plane. We conjecture that as $\alpha \rightarrow 0$, the number of eigenvalues in the right half plane tends to infinity. This further underscores the striking difference in the character of the problem when $\alpha > 0$ versus the case $\alpha = 0$.

2. Linear stability

In order to consider the linear stability of the traveling wave, we seek solutions of (1.1) in the form

$$u(x, t) = \phi(x - ct) + v(x - ct, t)$$

and neglect terms which are $\mathcal{O}(v^2)$. The linear evolution equation for the perturbation $v(\xi, t)$ is

$$\partial_t v = \mathcal{A}_\alpha v, \quad \mathcal{A}_\alpha = \partial_\xi [-\partial_\xi^2 + \alpha \partial_\xi + c - \phi(\xi)^p], \quad (2.1)$$

where $\xi = x - ct$. We intend to study transition to instability by examining the spectrum of \mathcal{A}_α as the parameters α , c and p are varied. We consider \mathcal{A}_α as an operator on $L^2(\mathbb{R})$ with domain $D(\mathcal{A}_\alpha) = H^3(\mathbb{R})$, the Sobolev space of functions with L^2 derivatives up to third order. Regarding the structure of the spectrum, we refer to Henry [12, Ch. 5]. The spectrum is the same in $L^p(\mathbb{R})$, $1 \leq p < \infty$, or in the space of bounded uniformly continuous functions on \mathbb{R} . The spectrum consists of *discrete spectrum* (isolated eigenvalues of finite multiplicity) and *essential spectrum* (everything else not in the resolvent set). Since $\phi(\xi)$ approaches constant limits 0 and u_L at an exponential rate as $\xi \rightarrow \pm\infty$ respectively, the essential spectrum is determined from that of the constant coefficient operators

$$\mathcal{A}_+ = \partial_\xi (-\partial_\xi^2 + \alpha \partial_\xi + c), \quad (2.2)$$

$$\mathcal{A}_- = \partial_\xi (-\partial_\xi^2 + \alpha \partial_\xi + c - u_L^p). \quad (2.3)$$

Let S_c^\pm denote the spectrum of \mathcal{A}_\pm . Using the Fourier transform, one finds that (since $u_L^p - c = pc$)

$$S_c^+ = \{\lambda: \lambda = -\alpha\tau^2 + i\tau(\tau^2 + c), \tau \in \mathbb{R}\}, \quad (2.4)$$

$$S_c^- = \{\lambda: \lambda = -\alpha\tau^2 + i\tau(\tau^2 - pc), \tau \in \mathbb{R}\}. \quad (2.5)$$

The sets S_c^+ and S_c^- are two curves in the closed left half plane. The complement of $S_c^+ \cup S_c^-$ consists of a number of disjoint connected components. Let Ω^+ denote the component which contains the right half plane. Then the essential spectrum can be characterized by the following result which is proved in [24].

Proposition 2.1. Let $\alpha > 0$. The essential spectrum of \mathcal{A}_α contains $S_c^+ \cup S_c^-$, but contains no point of the component Ω_+ . In particular, points in the spectrum of \mathcal{A}_α , lying in Ω_+ , must be isolated eigenvalues.

The situation is simpler for the case $\alpha = 0$, when $\phi(\xi)$ is replaced by $\phi_0(\xi)$, which tends to 0 as $\xi \rightarrow \pm\infty$. Let $\mathcal{A}_0 = \partial_\xi (-\partial_\xi^2 + c - \phi_0(\xi)^p)$. In this case the essential spectrum is $S_c^0 = \{\lambda: \lambda = i\tau(\tau^2 + c), \tau \in \mathbb{R}\}$, which is the imaginary axis.

Regarding the discrete spectrum of \mathcal{A}_0 , it has been shown in [24, theorem 3.4] that: For $p < 4$, \mathcal{A}_0 has no discrete eigenvalues λ with $\text{Re } \lambda \neq 0$. For $p > 4$, \mathcal{A}_0 has a pair of symmetrically placed eigenvalues $\pm\lambda_0(p) \in \mathbb{R}$, $\lambda_0 > 0$. Each of these eigenvalues is simple, having multiplicity one. As $p \downarrow 4$, the eigenvalue $\lambda_0(p) \rightarrow 0$, merging with the origin at the transition value $p = 4$. There are no other isolated eigenvalues λ with $\text{Re } \lambda \neq 0$. However, $\lambda = 0$ is an eigenvalue embedded in the essential spectrum of \mathcal{A}_0 , with eigenfunction $\partial_\xi \phi_0(\xi)$, associated with the translation invariance of (1.1). See fig. 2.

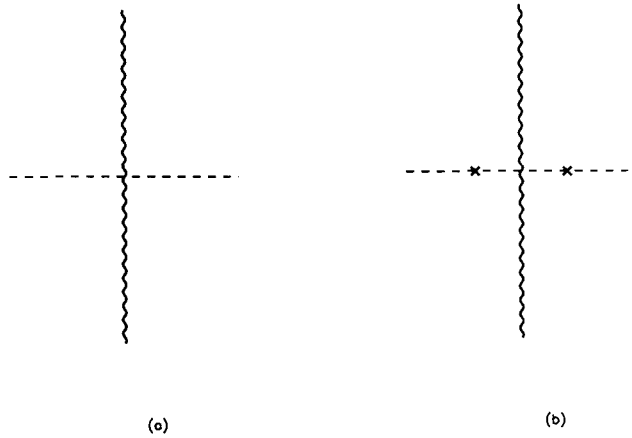


Fig. 2. Spectrum of \mathcal{A}_0 for (a) $p < 4$ and (b) $p > 4$. Wavy line indicates that the essential spectrum covers the imaginary axis.

Much less is known concerning the discrete spectrum of \mathcal{A}_α for $\alpha > 0$, in general. When $\alpha > 0$, $\lambda = 0$ is an eigenvalue of \mathcal{A}_α embedded in the essential spectrum, with eigenfunction $\partial_\xi \phi(\xi)$. From the considerations of section 1, we conjecture that for any $p > 4$ and c fixed, as $\alpha \rightarrow 0$ a transition to linear instability should occur via the appearance of one or more eigenvalues of \mathcal{A}_α in the right half plane. However, in [24] it was proved that the mechanism for such a transition to instability cannot be like that in the case $\alpha = 0$ – no eigenvalue may merge with the origin while α remains strictly positive. (See section 3.)

In this paper we show numerically, that a transition to instability does occur via a pair of complex conjugate eigenvalues crossing from the left half plane to the right half plane, as α decreases. There is additional evidence that more pairs of eigenvalues cross into the right half plane as α is decreased further. In fig. 3 we display some of the results of our numerical computations for $p = 6$, $c = 1$, and (a) $\alpha = 0.08$, (b) $\alpha = 0.07$. The solid curves correspond to the curves S_e^+ and S_e^- , which bound the essential spectrum of \mathcal{A}_α . (From (2.4)–(2.5) it is seen that S_e^+ and S_e^- approach the imaginary axis as α decreases toward zero.) In fig. 3b the crosses indicate isolated eigenvalues at $\lambda = 0.0667 \pm 1.985i$, for $\alpha = 0.07$. These eigenvalues are zeros of Evans’ function $D(\lambda)$, to be described below. In fig. 3a the crosses indicate the corresponding zeros of $D(\lambda)$ for $\alpha = 0.08$. As α decreases, these zeros move to the right,

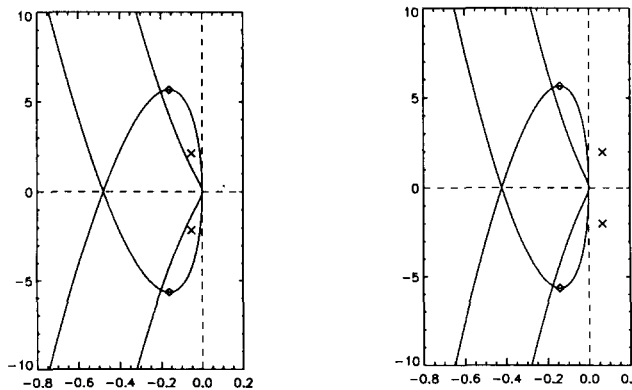


Fig. 3. Spectrum of \mathcal{A}_α for $p = 6$ and (a) $\alpha = 0.08$, (b) $\alpha = 0.07$. Crosses mark zeros of $D(\lambda)$, curves bound essential spectrum.

crossing first the curve S_c to become isolated eigenvalues in Ω_+ , then crossing the imaginary axis, indicating a transition to instability. The crossing appears to be transversal: we estimate that $\text{Re}(d\lambda/d\alpha) \approx -11.9$.

3. Evans' function and eigenvalues

The approach we use to determine the isolated eigenvalues of the operator \mathcal{A}_α in (2.1) is based on the numerical computation of Evans' function $D(\lambda)$, an analytic function whose zeros correspond to these isolated eigenvalues. J.W. Evans introduced $D(\lambda)$ in [8] to study the stability of nerve impulses. Evans and Feroe [9] numerically studied the linear stability of nerve impulse solutions of the Hodgkin–Huxley equations, by computing $D(\lambda)$ and locating its zeros using the argument principle. This is the method we shall use below. Recently, Swinton and Elgin [27] have used the same approach to study numerically the linear stability of laser pulses. Evans' function $D(\lambda)$ has also been used in a number of theoretical studies of traveling wave stability: for nerve impulses [8,16, 32], singularly perturbed reaction diffusion systems [1,10], flame fronts [28], and solitary waves [24].

In [24], the generalized KdV–Burgers equation (1.1) was also considered. We now summarize and extend the results of [24], that describe $D(\lambda)$ and its properties, for the traveling waves of (1.1).

If λ is an eigenvalue of \mathcal{A}_α with corresponding L^2 eigenfunction $Y(\xi)$, then Y is a solution of the differential equation

$$\partial_\xi[-\partial_\xi^2 + \alpha\partial_\xi + c - \phi(\xi)^p]Y(\xi) = \lambda Y(\xi). \quad (3.1)$$

As ξ tends to $\pm\infty$ respectively, the coefficients of (3.1) tend to those of the corresponding constant coefficient equations

$$\partial_\xi(-\partial_\xi^2 + \alpha\partial_\xi + c)Y(\xi) = \lambda Y(\xi), \quad (3.2)$$

$$\partial_\xi(-\partial_\xi^2 + \alpha\partial_\xi + c - u_1^p)Y(\xi) = \lambda Y(\xi). \quad (3.3)$$

These equations have solutions of the form $\exp(\mu\xi)$, where for (3.2) and (3.3) respectively, the exponent μ satisfies

$$\mathcal{P}_+(\mu) = \mu^3 - \alpha\mu^2 - c\mu + \lambda = 0, \quad (3.4a)$$

$$\mathcal{P}(\mu) = \mu^3 - \alpha\mu^2 + p c \mu + \lambda = 0. \quad (3.4b)$$

For an arbitrary $\lambda \in \Omega^+$, eqs. (3.4a,b) respectively have roots $\mu_j^+(\lambda)$, $j = 1, 2, 3$, which satisfy

$$\text{Re } \mu_1^+(\lambda) < 0 < \text{Re } \mu_j^+(\lambda), \quad j = 2, 3. \quad (3.5)$$

Corresponding to the solution $\exp(\mu_1^+\xi)$ of (3.2), which decays to zero as $\xi \rightarrow +\infty$, eq. (3.1) has a solution $Y^+(\xi, \lambda)$, which is analytic in λ and satisfies

$$Y^+(\xi, \lambda) \sim \exp(\mu_1^+\xi) \quad \text{as } \xi \rightarrow +\infty. \quad (3.6)$$

From this solution $Y^+(\xi, \lambda)$, one can define a function $D(\lambda)$, which is a sort of *transmission coefficient*, with the property that

$$Y^+(\xi, \lambda) \sim D(\lambda) \exp(\mu_1^- \xi) \quad \text{as } \xi \rightarrow -\infty. \quad (3.7)$$

$D(\lambda)$ is an analytic function in Ω^+ . If $D(\lambda) = 0$ for $\lambda \in \Omega^+$, then $Y^+(\xi, \lambda)$ must decay exponentially as $\xi \rightarrow -\infty$. In this case, λ is an eigenvalue of (3.1) with corresponding eigenfunction $Y^+(\xi, \lambda)$. Conversely, if λ is an eigenvalue with corresponding eigenfunction $Y(\xi)$, then $Y(\xi)$ must be a constant multiple of $Y^+(\xi, \lambda)$ and so $D(\lambda) = 0$, since $Y(\xi)$ is bounded on \mathbb{R} . Hence, we have:

Theorem 3.1. For $\lambda \in \Omega^+$, λ is an eigenvalue of \mathcal{A}_α is and only if $D(\lambda) = 0$.

The origin $\lambda = 0$ is an eigenvalue of \mathcal{A}_α with eigenfunction $\partial_\xi \phi$. But $\lambda = 0 \notin \Omega^+$, instead, zero is embedded in the essential spectrum of \mathcal{A}_α . So theorem 3.1 does not apply. It is useful to observe, therefore, that $D(\lambda)$ is naturally defined, by the same formula (3.7), on the larger domain $\Omega \supset \Omega^+$, which is defined by the requirements

$$\operatorname{Re} \mu_1^\pm(\lambda) < \operatorname{Re} \mu_j^\pm(\lambda), \quad j = 2, 3. \quad (3.8)$$

These inequalities hold in a region contained in Ω of the form $\{z: \operatorname{Re} z > -\epsilon_0\}$, for some $\epsilon_0 > 0$ depending on α, c and p . Note that

$$\begin{aligned} \mu_1^-(0) &= 0, & \mu_j^-(0) &= \frac{1}{2}(\alpha \pm i\sqrt{4pc - \alpha^2}), \quad j = 2, 3, \\ \mu_1^+(0) &= \frac{1}{2}(\alpha - \sqrt{\alpha^2 + 4c}) < \mu_2^+(0) = 0 < \mu_3^+(0) = \frac{1}{2}(\alpha + \sqrt{\alpha^2 + 4c}). \end{aligned}$$

Now it easily follows that: $D(0) = 0$.

When $\alpha > 2\sqrt{pc}$ and the wave profile $\phi(\xi)$ is monotone decreasing, the traveling wave $\phi(x - ct)$ can be shown to be nonlinearly stable, following the argument in [23] for the case $p = 1$. Correspondingly, the following linear stability result was proved in [24].

Proposition 3.2. Assume $\alpha > 2\sqrt{pc}$. Then $D(\lambda) \neq 0$ if $\operatorname{Re} \lambda > 0$.

For describing what happens as α is decreased, we note that for $\alpha > 0$ and $\lambda \in \Omega_+ = \Omega_+(\alpha)$, $D(\lambda) = D(\lambda, \alpha)$ is locally an analytic function of α . (This follows from [24], remark 1.12.) The following results will be useful.

Proposition 3.3. For $\alpha > 0$, $D(\lambda) \rightarrow 1$ as $|\lambda| \rightarrow \infty$ with $\lambda \in \Omega^+$, uniformly for $\alpha \in [a, b]$ for any $a, b > 0$.

Proposition 3.4. For any $\alpha > 0, p \geq 1, c > 0$ we have $D'(0) \neq 0$.

Proposition 3.3 will be proved in the appendix. The result of proposition 3.4 is proved in [24], but we briefly recall how the proof goes. First, by a method resembling Melnikov’s method (see [22,25]) for studying the order of contact of stable and unstable manifolds in perturbed autonomous systems of ODEs, an integral formula for $D'(\lambda)$ was proved, cf. formula (1.35) of [24]. Applied to the present problem, this formula yields

$$D'(0) = \int_{-\infty}^{\infty} Z^-(\xi, 0) Y^+(\xi, 0) d\xi,$$

where $Y^+(\xi, \lambda)$ is as described above (see (3.6)), and $Z^-(\xi, 0)$ is the unique solution of the 'transposed' equation

$$0 = (-\partial_{\xi}^2 - \alpha \partial_{\xi} + c - \phi^p) \partial_{\xi} Z^-,$$

such that

$$Z^-(\xi, 0) \rightarrow 1/\mathcal{P}'(0) = 1/pc \quad \text{as } \xi \rightarrow -\infty.$$

Indeed, $Z^-(\xi, 0)$ is simply constant, and using (1.6) we find

$$Z^-(\xi, 0) = 1/pc, \quad Y^+(\xi, 0) = \nu^{-1} e^{\nu\xi_0} \partial_{\xi} \phi(\xi).$$

Therefore

$$D'(0) = \frac{e^{\nu\xi_0}}{\nu pc} \int_{-\infty}^{\infty} 1 \cdot \partial_{\xi} \phi(\xi) d\xi = \frac{-e^{\nu\xi_0} u_1}{\nu pc} \neq 0.$$

Using the results above, we find that, *assuming* instability occurs for some sufficiently small $\alpha > 0$, transition to instability must be associated with the existence of complex conjugate eigenvalues on the imaginary axis:

Theorem 3.5. Suppose that for some $\alpha_1 > 0$ we have $D(\lambda_1, \alpha_1) = 0$ for some λ_1 with $\text{Re } \lambda_1 > 0$. Let

$$\alpha_* = \sup\{\alpha \mid \alpha > 0 \text{ and } D(\lambda, \alpha) = 0 \text{ for some } \lambda \text{ with } \text{Re } \lambda > 0\}.$$

Then $0 < \alpha_* < 2\sqrt{pc}$, and there exists λ_* with $\text{Re } \lambda_* = 0$ but $\lambda_* \neq 0$, such that $D(\lambda_*, \alpha_*) = 0$. Hence, \mathcal{A}_{α_*} has a pair of nonzero purely imaginary complex conjugate eigenvalues $\lambda_*, \overline{\lambda_*}$.

Proof. Suppose that for some $\alpha > 0$, $D(\lambda)$ has one or more zeros in the right half plane $\text{Re } \lambda > 0$, so $\alpha_* > 0$. From proposition 3.2 it follows $\alpha_* < 2\sqrt{pc}$. Now there exists a sequence $\{\alpha_j\}_{j=1}^{\infty}$, with $\alpha_j > 0$ and $\lim_{j \rightarrow \infty} \alpha_j = \alpha_*$, such that \mathcal{A}_{α_j} has an eigenvalue λ_j with $D(\lambda_j, \alpha_j) = 0$ and $\text{Re } \lambda_j > 0$ for all j . By proposition 3.3 the sequence $\{\lambda_j\}$ is bounded. Passing to a subsequence, we may assume $\lim_{j \rightarrow \infty} \lambda_j = \lambda_*$ exists. Then $D(\lambda_*, \alpha_*) = 0$, and we have $\text{Re } \lambda_* = 0$. (If $\text{Re } \lambda_* > 0$ then by continuity $D(\lambda, \alpha) = 0$ for some λ, α with $\alpha > \alpha_*$, $\text{Re } \lambda > 0$, contradicting the definition of α_* .)

Now, we have $D(\lambda_j, \alpha_j) = 0 = D(0, \alpha_j)$. If $\lambda_* = 0$, then it follows from Rouché's theorem that $\lambda = 0$ is a zero of $D(\lambda, \alpha_*)$ of order at least two, which implies $D'(0) = 0$. This contradicts proposition 3.4. So λ_* must be purely imaginary and nonzero. \square

Remark. Note that in the proof above, it would have been natural to guess that $\lambda_* = 0$, since that is what happens in the transition to instability for the solitary wave $\phi_0(x - ct)$ of the gKdV equation as the

parameter p is varied with $\alpha = 0$: \mathcal{A}_0 admits an eigenvalue $\lambda_0(p) > 0$ for $p > 4$ with $\lambda_0(p) \rightarrow 0$ as $p \rightarrow 4$ [24]. However, such a scenario is precluded when $\alpha > 0$ by the result of proposition 3.4.

The result of theorem 3.5 motivates us to try to demonstrate that a transition to instability does occur, by searching computationally for complex zeros of $D(\lambda)$ crossing into the right half plane as α decreases. In section 4, we will use the argument principle to count the number of zeros of $D(\lambda)$ in the right half plane. For that purpose, we now discuss the original characterization of $D(\lambda)$ given by Evans [8], which leads to a more efficient algorithm for computing $D(\lambda)$ than is suggested by (3.7). To describe this characterization, we follow the development of [24].

First, write (3.1) as a system of three first order ODE's, using the standard reduction: $y = (Y, Y', Y'')^t$. We have

$$\frac{dy}{d\xi} = A(\xi, \lambda) y,$$

where

$$A(\xi, \lambda) = \begin{pmatrix} 0 & 1 & 0 \\ 0 & 0 & 1 \\ -\lambda - \partial_\xi \phi(\xi)^p & c - \phi(\xi)^p & \alpha \end{pmatrix}. \quad (3.9)$$

We are also interested in the adjoint equation:

$$\frac{dz}{d\xi} = -zA(\xi, \lambda), \quad (3.10)$$

where $z(\xi)$ is a 3-component row vector. The quantities $\mu_j^\pm(\lambda)$ in (3.5) are eigenvalues of the asymptotic matrices

$$A^\pm(\lambda) = \lim_{\xi \rightarrow \pm\infty} A(\xi, \lambda).$$

The inequality (3.8) ensures the existence of solutions $\zeta^+(\xi, \lambda)$ of (3.9) and $\eta^-(\xi, \lambda)$ of (3.10), analytic in λ for $\lambda \in \Omega$, such that

$$\zeta^+(\xi, \lambda) \sim \exp(\mu_1^+ \xi) v^+ \quad \text{as } \xi \rightarrow +\infty, \quad (3.11)$$

$$\eta^-(\xi, \lambda) \sim \exp(-\mu_1^- \xi) w^- \quad \text{as } \xi \rightarrow -\infty. \quad (3.12)$$

Here we make use of the definitions

$$v^+ = \begin{pmatrix} 1 \\ \mu_1^+ \\ (\mu_1^+)^2 \end{pmatrix}, \quad v^- = \begin{pmatrix} 1 \\ \mu_1^- \\ (\mu_1^-)^2 \end{pmatrix}, \quad (3.13)$$

$$w^+ = (\mu_1^+(\mu_1^+ - \alpha) - c, \mu_1^+ - \alpha, 1) / \mathcal{P}'_+(\mu_1^+), \quad (3.14a)$$

and

$$w^- = (\mu_1^-(\mu_1^- - \alpha) + \rho c, \mu_1^- - \alpha, 1) / \mathcal{P}'_-(\mu_1^-), \quad (3.14b)$$

which satisfy

$$(A^\pm - \mu_1^\pm I)v^\pm = 0, \quad w^\pm(A^\pm - \mu_1^\pm I) = 0, \quad w^+v^+ = w^-v^- = 1. \quad (3.15)$$

If y and z are any solutions to (3.9) and (3.10), then it is easy to check that $z \cdot y$ is independent of ξ . Using the particular choices $z = \eta^-(\xi, \lambda)$, and $y = \zeta^+(\xi, \lambda)$, we have using proposition 1.4 of [24] that

$$\zeta^+(\xi, \lambda) \sim (\eta^- \cdot \zeta^+)(\lambda) \exp(\mu_1^-\xi) v^-(\lambda) \quad \text{as } \xi \rightarrow -\infty. \quad (3.16)$$

Comparison of the first component of (3.16) with (3.7) yields the formula

$$D(\lambda) = (\eta^- \cdot \zeta^+)(\lambda). \quad (3.17)$$

4. Computational search for eigenvalues

Our strategy is summarized as follows. By theorem 3.1, the search for eigenvalues of \mathcal{A}_α , the operator in (2.1), is reduced to the search for zeros of $D(\lambda)$. Zeros of $D(\lambda)$ in the right half plane can be counted using the argument principle. Since for $\text{Re } \lambda \geq 0$, $D(\lambda) \rightarrow 1$ as $|\lambda| \rightarrow \infty$, it follows that the number of zeros in the right half plane is determined by the number of times the image of the imaginary axis $\{z: z = it, t \in \mathbb{R}\}$ under $D(\cdot)$ wraps around the origin. Taking into account that this axis contains $\lambda = 0$, a simple zero of $D(\lambda)$, we find the following expression for n^+ , the number of zeros of $D(\lambda)$ with $\text{Re } \lambda > 0$:

$$n^+ = -\frac{1}{2\pi} \int_{-\infty}^{+\infty} \frac{D'(it)}{D(it)} dt - \frac{1}{2}. \quad (4.1)$$

The quantity $n^+ + \frac{1}{2}$ is the winding number of the curve $t \mapsto D(-it)$, $-\infty < t < +\infty$, with respect to the origin. This is the image under $D(\cdot)$ of the imaginary axis oriented in the positive sense relative to the right half plane. Since $\overline{D(\bar{\lambda})} = D(\bar{\lambda})$, this can be expressed in terms of the change in the argument of $D(it)$, as t varies from 0^+ to $+\infty$:

$$n^+ = \frac{1}{\pi} [\arg D(+i \cdot 0) - \arg D(+i \cdot \infty)] - \frac{1}{2}. \quad (4.2)$$

Our numerical strategy to evaluate n^+ is to evaluate $D(it)$ for values of t ranging from 0.005 to 300 000, minimizing computation by adaptively changing the increment in t , while keeping the angle between successive segments within prescribed bounds. The argument of $D(it)$ is updated from step to step, so that n^+ can be evaluated using formula (4.2) at the end of the computation.

For computing, we introduce the variable $v(\xi, \lambda) = \exp[-\mu_1(\xi, \lambda)\xi] \zeta^-(\xi, \lambda)$, cf. (3.9), where

$$\mu_1(\xi, \lambda) = \begin{cases} \mu_1^+ & \text{for } \xi > 0, \\ \mu_1^- & \text{for } \xi < 0. \end{cases} \quad (4.3)$$

The function $v(\xi, \lambda)$ satisfies

$$\frac{dv}{d\xi} = [A(\xi, \lambda) - \mu_1 I]v, \tag{4.4}$$

$$v(\xi, \lambda) \rightarrow \begin{cases} v^+ & \text{as } \xi \rightarrow +\infty, \\ D(\lambda)v^- & \text{as } \xi \rightarrow -\infty. \end{cases} \tag{4.5}$$

Let $w(\xi, \lambda) = \exp[\mu_1(\xi, \lambda)\xi] \eta^-(\xi, \lambda)$. Then, $D(\lambda) = w \cdot v$ and w satisfies

$$\frac{dw}{d\xi} = -w(A(\xi, \lambda) - \mu_1 I), \quad w(\xi, \lambda) \rightarrow w^- \text{ as } \xi \rightarrow -\infty.$$

To approximate $D(\lambda)$ numerically, we fix $\xi_+ > 0$ large, and solve (4.4) by a 4th order Runge–Kutta method, setting $v(\xi_+) = v^+$. The system (4.4) is solved simultaneously with the system describing the wave profile, $\phi(\xi)$:

$$\frac{d\phi}{d\xi} = \psi, \quad \frac{d\psi}{d\xi} = \alpha\psi + c\phi - \frac{1}{p+1} \phi^{p+1}. \tag{4.6}$$

Since from (1.6), $(\phi, \psi) \sim e^{\nu(\xi-\xi_0)}(1, \nu)$ as $\xi \rightarrow +\infty$, we fix the phase of the wave by setting $\xi_0 = 0$ and approximate by imposing the initial condition

Table 1
Comparison of two approximations of $D(\lambda)$.

ξ	$\phi(\xi)$	$v_1(\xi)$	$w^- \cdot v(\xi)$
-200.0	1.382 78	-0.017 043 - 0.002 920i	-0.011 739 - 0.000 313i
-200.2	1.382 77	-0.015 799 + 0.003 097i	-0.011 738 - 0.000 305i
-200.4	1.382 83	-0.012 580 + 0.007 822i	-0.011 729 - 0.000 301i
-200.6	1.382 95	-0.008 514 + 0.009 940i	-0.011 718 - 0.000 306i
-200.8	1.383 10	-0.005 081 + 0.008 994i	-0.011 712 - 0.000 314i
-201.0	1.383 25	-0.003 600 + 0.005 495i	-0.011 709 - 0.000 318i
-201.2	1.383 35	-0.004 763 + 0.000 719i	-0.011 705 - 0.000 314i
-201.4	1.383 40	-0.008 376 - 0.003 739i	-0.011 698 - 0.000 306i
-201.6	1.383 37	-0.013 406 - 0.006 497i	-0.011 692 - 0.000 301i
-201.8	1.383 27	-0.018 304 - 0.006 832i	-0.011 695 - 0.000 303i
-202.0	1.383 13	-0.021 513 - 0.004 883i	-0.011 708 - 0.000 307i
-202.2	1.382 99	-0.021 980 - 0.001 563i	-0.011 725 - 0.000 309i
-202.4	1.382 87	-0.019 498 + 0.001 798i	-0.011 736 - 0.000 308i
-202.6	1.382 80	-0.014 779 + 0.003 924i	-0.011 736 - 0.000 305i
-202.8	1.382 80	-0.009 226 + 0.004 046i	-0.011 728 - 0.000 307i
-203.0	1.382 87	-0.004 484 + 0.002 154i	-0.011 720 - 0.000 311i
-348.6	1.383 09	-0.011 683 - 0.000 314i	-0.011 714 - 0.000 309i
-348.8	1.383 09	-0.011 696 - 0.000 334i	-0.011 714 - 0.000 309i
-349.0	1.383 09	-0.011 716 - 0.000 345i	-0.011 714 - 0.000 309i
-349.2	1.383 09	-0.011 737 - 0.000 343i	-0.011 714 - 0.000 309i
-349.4	1.383 09	-0.011 750 - 0.000 331i	-0.011 714 - 0.000 309i
-349.6	1.383 09	-0.011 753 - 0.000 312i	-0.011 714 - 0.000 309i
-349.8	1.383 09	-0.011 743 - 0.000 294i	-0.011 714 - 0.000 309i
-350.0	1.383 09	-0.011 724 - 0.000 282i	-0.011 714 - 0.000 309i

$$(\phi(\xi_+), \psi(\xi_+)) = \exp(\nu\xi_+) (1, \nu). \tag{4.7}$$

The direction of decreasing ξ is the stable direction for integrating (4.4) and (4.6), in order to approximate the stable manifold of the saddle point $(0, 0)$ in (4.6), and to compute the solution spanning the stable subspace for system (4.4). We integrate (4.4) and (4.6) for $\xi_+ > \xi > \xi_-$, where $\xi_- < 0$ is sufficiently large so that $(\phi(\xi_-), \psi(\xi_-))$ is approximately equal to $(u_L, 0)$. When this holds, $w(\xi_-, \lambda) \sim w^-$, and therefore $D(\lambda)$ is given approximately by

$$D(\lambda) \sim w^- \cdot v(\xi_-, \lambda). \tag{4.8}$$

Remark. The approximation (4.8) turns out to be rather better than the approximation $D(\lambda) \sim v_1(\xi_-, \lambda)$ suggested by (4.5). Apparently, this is because the rate of convergence in (4.5) as $\xi \rightarrow -\infty$ can be rather slow. But the slowly decaying components of $v(\xi, \lambda)$ are orthogonal to $w(\xi, \lambda)$, so are eliminated by (4.8) if the approximation $w(\xi_-, \lambda) \sim w^-$ is good. In table 1 we list some computed values of $v_1(\xi)$ and $w^- \cdot v(\xi)$ for parameters near the transition to instability: $p = 6, c = 1, \alpha = 0.074, \lambda = 2i$. Discretization error is estimated to be of the order of 10^{-7} for this computation, which was performed with $\xi_+ = 5$, and step size $\Delta\xi = 0.01$.

4.1. Numerical results

In our numerical computations, we fix $c = 1$, so $u_L = (p + 1)^{1/p}$. Results for other values of c may be recovered from the scaling satisfied by the wave profile, namely

$$\phi(\xi, c, p, \alpha) = c^{1/p} \phi(c^{1/2}\xi, 1, p, c^{-1/2}\alpha). \tag{4.9}$$

In fig. 4 we plot $\pi^{-1} \arg D(it)$ versus t for $p = 6$ and the cases $\alpha = 0.074$ (dashed line) and $\alpha = 0.077$ (dash-dotted). From (4.2), for $\alpha = 0.077$ we find $n^+ = 0$, i.e., there are no eigenvalues of positive real part. But for $\alpha = 0.074$, we find $n^+ = 2$ indicating that there are 2 eigenvalues of positive real part.

Figure 5 shows a portion of the curve $t \mapsto D(it)$, $-\infty < t < \infty$, for the cases (a) $\alpha = 0.077$, and (b) $\alpha = 0.074$. As α decreases from $\alpha = 0.077$ to $\alpha = 0.074$, we see that the loops around $\lambda = 0$ in fig. 5a deform, so that they no longer pass around $\lambda = 0$ in fig. 5b. The rest of the curve changes little from

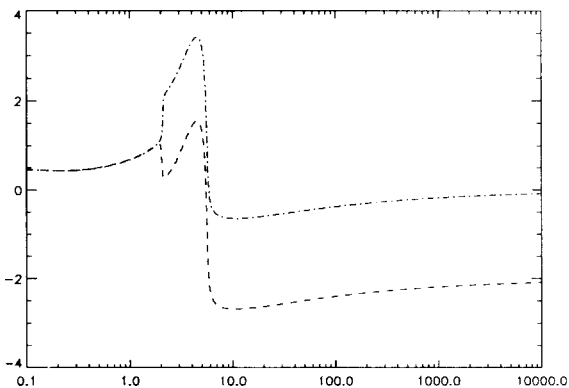


Fig. 4. $\pi^{-1} \arg D(it)$ versus t for $p = 6$, $\alpha = 0.074$ (dashed), $\alpha = 0.077$ (dash-dotted).

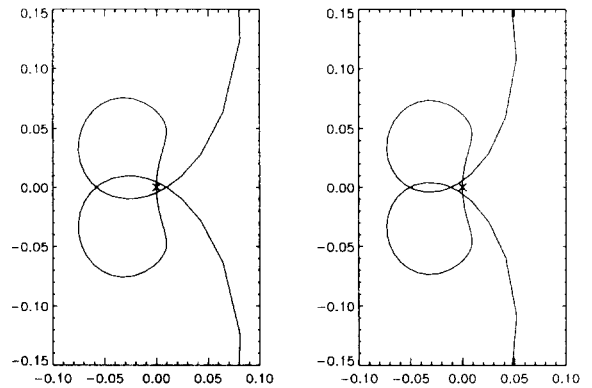


Fig. 5. The curve $D(it)$ near the origin, for $p = 6$. (a) $\alpha = 0.077$, (b) $\alpha = 0.074$.

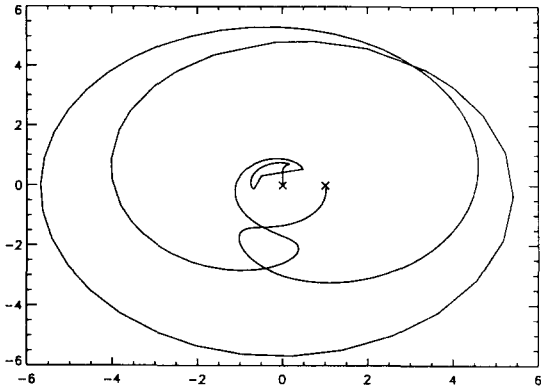


Fig. 6. The curve $D(it)$, for $p = 6$, $\alpha = 0.074$. The magnitude $|D(it)|$ is scaled by taking the tenth root.

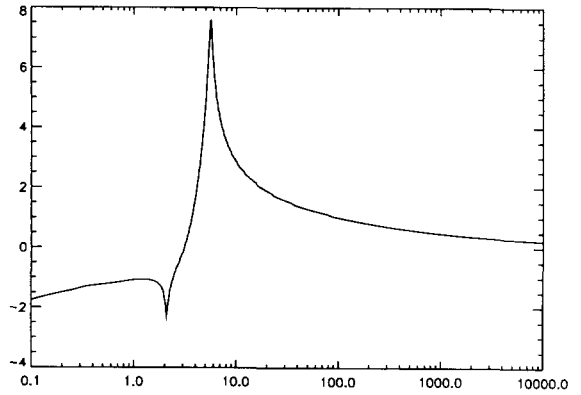


Fig. 7. $\log_{10}|D(it)|$ versus t for $p = 6$, $\alpha = 0.074$.

case (a) to case (b), so we see that the total change in the winding number in (4.1) is $+2$ as α decreases from 0.077 to 0.074.

In fig. 6, we plot the image under $D(\cdot)$ of the upper half of the imaginary axis, the curve $t \mapsto D(it)$, $0 < t < \infty$. Because of the large variation in the magnitude of $D(it)$ (see fig. 7), the tenth root of the magnitude is taken; thus fig. 6 is a polar plot of $|D(it)|^{1/10}$ versus $\arg D(it)$. The large spike in the magnitude of $D(it)$ appears to be associated with proximity to the point λ_* on the boundary of the domain Ω where $\mu_1^-(\lambda_*) = \mu_2^-(\lambda_*)$. Since $\mathcal{P}'_-(\mu) = 0$ at this point, one finds that

$$\lambda_* = -\mu^3 + \alpha\mu^2 - p\mu, \quad \mu = \mu_1^-(\lambda_*) = \frac{1}{3}(\alpha + i\sqrt{3p - \alpha^2}).$$

This point is plotted as a diamond in fig. 3; it is close to the curve S_c^- because α is small.

For $p = 6$, the transition to instability occurs at approximately $\alpha = 0.075596$. The eigenvalues cross the imaginary axis at approximately $\lambda = \pm 2.0695i$. We also computed that a second pair of eigenvalues cross into the right half plane at $\alpha = 0.03657$, with $\lambda = \pm 2.2579i$. There is evidence that a third pair crosses as α is decreased further. We conjecture that, given any N , there is an α_N such that for $\alpha < \alpha_N$, N pairs of eigenvalues have crossed into the right half plane, with $\alpha_N \rightarrow 0$ as $N \rightarrow \infty$.

We plot in fig. 8 some parts of the curves α versus p along which the real part of some eigenvalue is

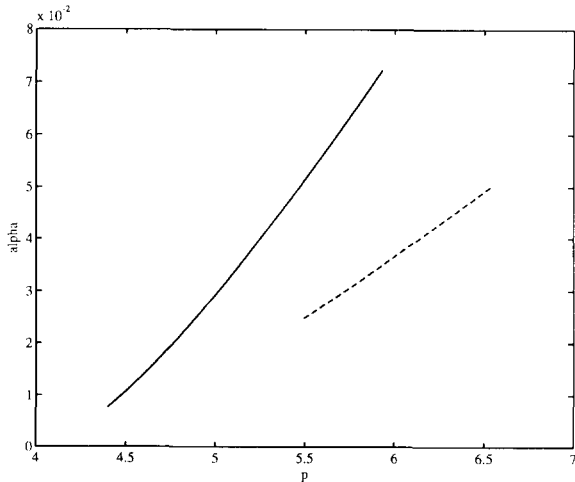


Fig. 8. Transition curves, where $\text{Re } \lambda = 0$ for some eigenvalue.

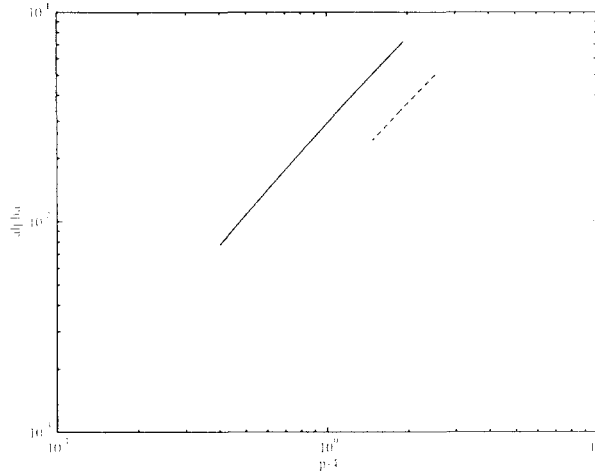


Fig. 9. Transition curves $\alpha_j(p)$ versus $p - 4$, log-log plot.

zero. The upper curve marks the neutral stability curve $\alpha = \alpha_0(p)$, across which the transition to instability occurs: n^+ jumps from 0 to 2 as α decreases across this curve. Across the lower curve $\alpha = \alpha_1(p)$, n^+ jumps from 2 to 4; a second complex conjugate pair of eigenvalues has crossed the imaginary axis.

As p decreases toward the value 4, the value of $\alpha = \alpha_0(p)$ along the neutral stability curve also decreases, as does the value of $\alpha = \alpha_1(p)$ along the second transition curve. Our numerical results are consistent with the hypothesis that $\alpha_0(p) \rightarrow 0$ as $p \downarrow 4$. It appears that the traveling wave $\phi(x - ct)$ is linearly stable for any $\alpha > 0$ when $p < 4$ (the regime where the solitary wave $\phi_0(x - ct)$ is stable). In fig. 9 we plot $\log \alpha_j(p)$ versus $\log(p - 4)$. We find that these graphs are nearly linear, with slope approaching $+\frac{3}{2}$ as $p \rightarrow 4^+$. Thus it appears that

$$\alpha_j(p) \sim K_j \cdot (p - 4)^{3/2} \quad \text{as } p \rightarrow 4^+, \quad (4.10)$$

where K_0 is approximately 0.031, and K_1 is approximately 0.014.

5. Dynamic simulations

We have performed numerical computations of solutions of the initial value problem for the generalized KdV-Burgers equation (1.1), with initial data close to a traveling wave, for parameter values near the transition to instability. The goal was to confirm the predictions of linear stability calculations in section 4, and to study the nature of the Hopf bifurcation suggested by the crossing of pairs of complex eigenvalues into the right half plane.

In order to describe the numerical scheme we used, first consider the evolution equation for the perturbation of the wave, $v(x - ct, t) = u(x, t) - \phi(x - ct)$, namely

$$\partial_t v = -\partial_\xi^3 v + \alpha \partial_\xi^2 v + c \partial_\xi v - \partial_\xi g(\xi, v) = \mathcal{A}_\alpha v - \partial_\xi g(\xi, v), \quad (5.1)$$

where

$$g(\xi, v) = \frac{1}{p+1} \{[\phi(\xi) + v]^{p+1} - \phi(\xi)^{p+1}\}.$$

We approximate the solution of (5.1) using Strang splitting [26]; in particular we solve with alternating fractional time steps of length Δt the equations

$$\partial_t v = \mathcal{A}_+ v, \tag{5.2}$$

$$\partial_t v + \partial_\xi g(\xi, v) = 0, \tag{5.3}$$

taking half-steps of length $\frac{1}{2} \Delta t$ at the beginning and end. We solve eq. (5.2) on a large finite interval $[\xi_-, \xi_+] = [-300, 20]$, using centered differences in ξ , and a Crank–Nicholson discretization in time. We used 256 00 grid points in space, with time step $\Delta t = 0.0005$. The boundary conditions imposed correspond to $v(\xi_-) = 0$, $v(\xi_+) = 0$, and $\partial_\xi v(\xi_+) = 0$. Equation (5.3) was solved using a Lax–Wendroff method [20]. The overall scheme is formally second order accurate in space and time.

Computations were performed for $p = 6$ and $\alpha = 0.05$ fixed, varying c near the value $c_{cr} \sim 0.438$, at which the transition to instability occurs. At this transition, a critical eigenvalue $\lambda_0(c)$ crossed into the right half plane, with $\lambda_0(c_{cr}) \sim 0.600i$.

For each calculation, the initial data was chosen as a small multiple of the eigenfunction corresponding to the critical eigenvalue:

$$v(\xi, 0) = \epsilon \operatorname{Re} Y^+(\xi, \lambda_*(c_{cr})) \tag{5.4}$$

for some $\epsilon > 0$. The real and imaginary parts of the eigenfunction $Y^+(\xi, \lambda_*(c_{cr}))$ at transition are plotted in fig. 10.

Results appear in figs. 11–16. For $c = 0.41$, the critical eigenvalue $\lambda(0.41) \sim -0.00777 + 0.553i$.

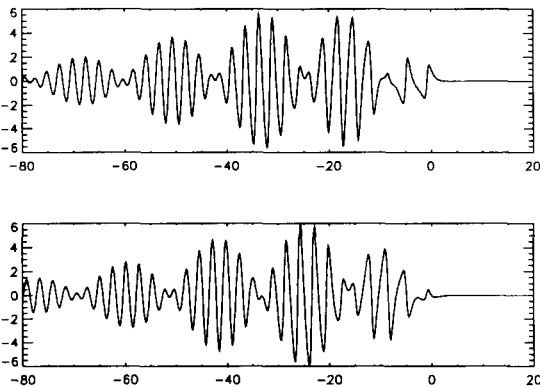


Fig. 10. Real (top) and imaginary (bottom) parts of the critical eigenfunction.

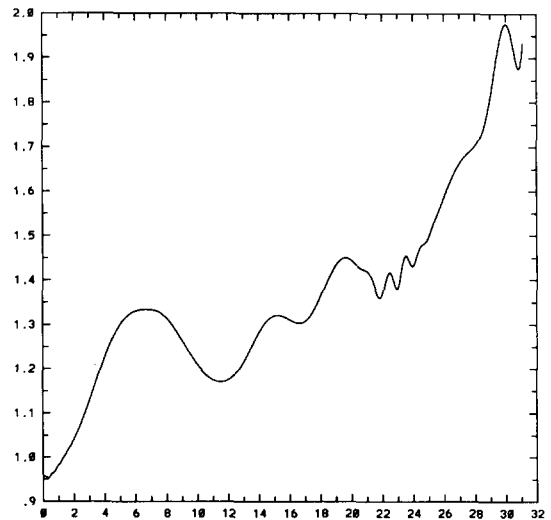


Fig. 11. L^2 norm of v versus t , for $c = 0.41$, $\epsilon = 0.05$.

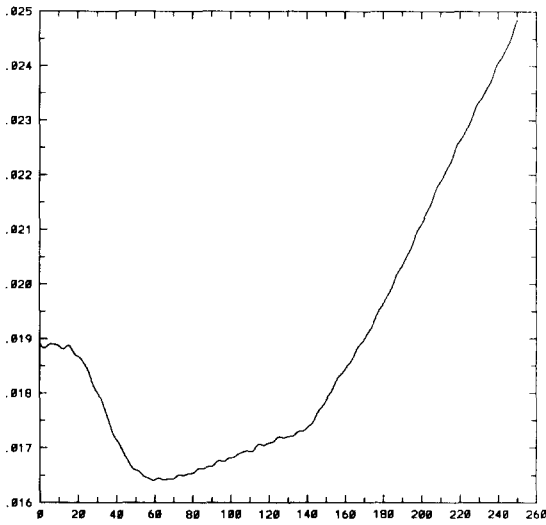


Fig. 12. L^2 norm of v versus t , for $c = 0.438$, $\epsilon = 0.001$.

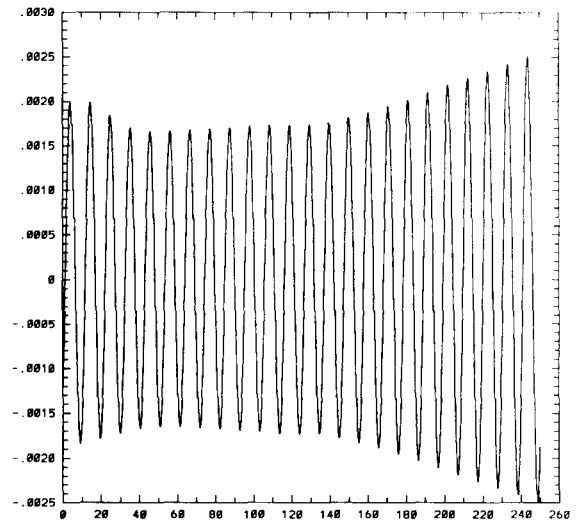


Fig. 13. $v(\xi_0, t)$ versus t , for $c = 0.438$, $\epsilon = 0.001$, $\xi_0 = -16$.

Choosing $\epsilon = 10^{-5}$, the L^2 norm of the solution for $0 < t < 50$ decayed toward zero at the rate $\exp(-0.0075t)$, agreeing well with the rate predicted by the linear stability calculation.

But when the perturbation amplitude ϵ is increased beyond $\epsilon = 0.05$, decay is no longer observed; a nonlinear instability occurs. The L^2 norm of the perturbation grows, and a complicated transient ensues. (See fig. 11.)

In figs. 12,13 appear results for the case $c = 0.438$, very close to but slightly above the predicted transition. As shown in fig. 12, for $\epsilon = 10^{-3}$ the L^2 norm of v is initially irregular, then increases

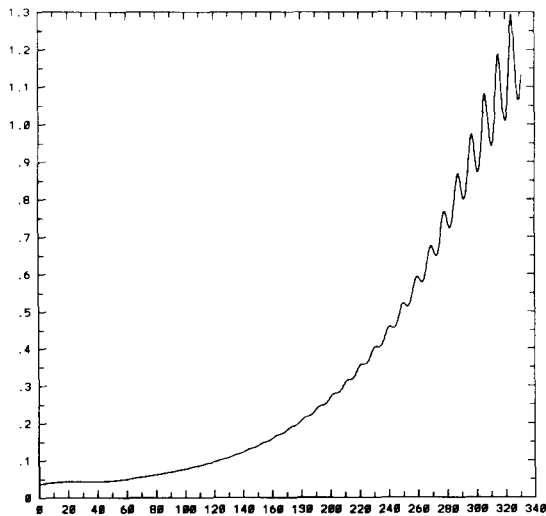


Fig. 14. L^2 norm of $v(\cdot, t)$ versus t , for $c = 0.47$, $\epsilon = 0.002$.

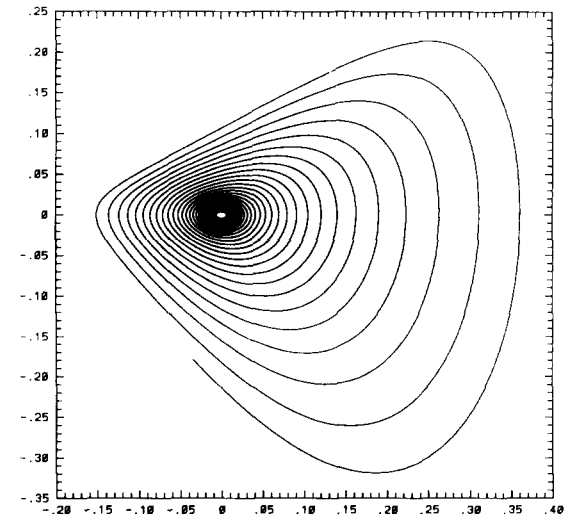


Fig. 15. $\partial_t v(\xi_0, t)$ versus $v(\xi_0, t)$, for $c = 0.47$, $\epsilon = 0.002$.

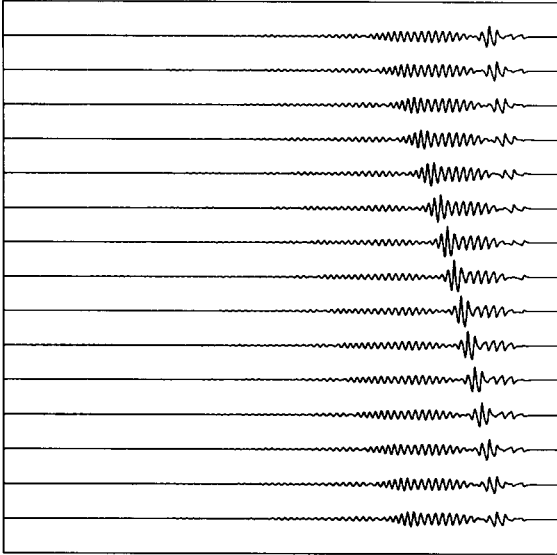


Fig. 16. $v(\xi, t)$ versus ξ , for $c = 0.47$, $\epsilon = 0.002$, $t = 319, \dots, 330$.

monotonically. A plot of $v(\xi_0, t)$ for ξ_0 fixed appears in fig. 13. For $c = 0.47$ the wave appears to be unstable. When $\epsilon = 10^{-5}$, the growth rate again agrees well with linear prediction. Taking $\epsilon = 0.002$, and computing for $0 < t < 330$, the perturbation is observed to grow to large amplitude. In fig. 14 we plot the L^2 norm of v versus t . In fig. 15, we plot $\partial_t v(\xi_0, t)$ versus $v(\xi_0, t)$. In fig. 16, we plot $v(\xi, t)$ versus ξ at integer times from $t = 319$ to 330 . Time increases upwards. The horizontal axis runs from -300 to 20 and the snapshots are successively displaced one unit upward along the vertical axis. This sequence illustrates how the perturbation is evolving as its magnitude begins to be comparable to that of the wave profile. An instability grows out of the leading part of the wave, propagates backward along the profile, then dissipates as a new cycle begins.

6. Conclusions

We have investigated the stability of traveling wave solutions of the generalized KdV–Burgers equation (1.1), by numerically finding eigenvalues using their characterization as zeros of Evans' function $D(\lambda)$, and by numeric integration of the initial value problem for perturbations of the wave.

To summarize the numerical evidence from section 4, a transition to linear instability takes place when:

- (a) For fixed positive c and $p > 4$, α is made sufficiently small;
- (b) For fixed positive α and $p > 4$, c is made sufficiently large.
- (c) For fixed positive α and c , p is made sufficiently large.

The transition to instability occurs as a pair of complex conjugate eigenvalues crosses the imaginary axis into the right half plane. This mechanism differs from that which occurs for the gKdV solitary wave

$\phi_0(x - ct)$ when $\alpha = 0$ and p increases past the critical value $p_{cr} = 4$. For $\alpha > 0$, additional pairs of complex eigenvalues cross into the right half plane as α is decreased or c is increased further. The neutral stability curve $\alpha = \alpha_0(p)$ is approximately described for p close to 4 by $\alpha_0(p) \sim 0.031(p - 4)^{3/2}$.

The numerical evidence in section 5 strongly suggests that a subcritical Hopf bifurcation occurs as c increases near $c_{cr} = 0.438$ (with $\alpha = 0.05$ and $p = 6$ fixed). No stable time periodic solution is detected. While we are not aware that a Hopf bifurcation theorem has been proved for eq. (5.1) for the evolution of perturbations of the traveling wave, the numerical results are consistent with a classical description of a subcritical Hopf bifurcation in finite dimensions [21]. They suggest the existence of an unstable time periodic solution which exists for $c < c_{cr}$, whose unstable manifold, of dimension two, contains a component in which solution trajectories spiral toward the origin $v = 0$, and a component on which the perturbation v grows to large amplitude. Thus the basin of attraction of the wave ϕ shrinks as c approaches c_{cr} , vanishing entirely for $c > c_{cr}$, when small perturbations grow to large amplitude.

We do not have analytical results to support the numerical evidence for instability, but it may be that in the limit $p \rightarrow 4$, $\alpha \rightarrow 0$, the eigenvalue problem may be accessible to analysis. The structure of the traveling wave can probably be well-characterized in that limit by studying the system (4.5) using the method of averaging and homoclinic bifurcation theory. (An asymptotic study was done for the KdV–Burgers equation with small α by Johnson [14].) More difficult (and interesting) would be characterizing Evans' function in the limit.

Appendix

Here we prove that $\lim_{\lambda \rightarrow \infty} D(\lambda) = 1$ for $\lambda \in \Omega_+$, which is proposition 3.3. The proof relies on results contained in §1.7 of [24]. Below, the proof is sketched out; for full details the reader is referred to [24].

For $|\lambda|$ large when $\lambda \in \Omega_+$, we will see below that the asymptotic matrices $A^\pm(\lambda)$ are diagonalizable. Define $V^\pm(\lambda)$ to be the matrix of right eigenvectors of $A^\pm(\lambda)$, with components $V_{jk}^\pm = (\mu_k^\pm)^{j-1}$. Define $W^\pm(\lambda)$ to be the corresponding matrix of left eigenvectors, with $W^\pm V^\pm = I$, so that $B^\pm(\lambda) = W^\pm A^\pm V^\pm = \text{diag}(\mu_1^\pm, \mu_2^\pm, \mu_3^\pm)$ is diagonal.

Define $p(\xi, \lambda) = W^+(\lambda) \zeta^+(\xi, \lambda)$, and $q(\xi, \lambda) = \eta^-(\xi, \lambda) V^-(\lambda)$. Then

$$dp/d\xi = B^+(\lambda)p + F^+(\xi, \lambda)p, \quad \xi > 0, \quad (\text{A.1})$$

$$dp/d\xi = -qB^-(\lambda) - qF^-(\xi, \lambda), \quad \xi < 0, \quad (\text{A.2})$$

where it turns out that the components of $F^\pm(\xi, \lambda)$ are given by

$$F_{jk}^\pm(\xi, \lambda) = [\rho_0(\xi) + \mu_k^\pm(\lambda) \rho_1^\pm(\xi)] / \mathcal{P}_\pm'(\mu_i^\pm(\lambda)),$$

with $\rho_0 = -\partial_\xi(\phi^p)$, $\rho_1^+ = -\phi^p$ and $\rho_1^- = (p+1)c - \phi^p$.

Now, from proposition 1.17 and corollary 1.19 of [24], we know that as $|\lambda| \rightarrow \infty$ with $\lambda \in \Omega_+$, $q(0, \lambda)$ is bounded and

$$p(0, \lambda) = W^+ \zeta^+(0, \lambda) = e_1 + o(1), \quad (\text{A.3})$$

$$q(0, \lambda) \cdot e_1 = \eta^-(0, \lambda) V^- e_1 = 1 + o(1), \quad (\text{A.4})$$

where $e_1 = (1, 0, 0)^t$, provided the following is true for $i = 0, 1$:

$$|(\mu_k^\pm)^j / \mathcal{P}'_\pm(\mu_j^\pm)| \leq C \quad \text{for } j = 1, 2, 3, k = 2, 3, \quad (\text{A.5})$$

$$|(\mu_1^\pm)^j / \mathcal{P}'_\pm(\mu_j^\pm)| = o(1) \quad \text{as } |\lambda| \rightarrow \infty, \text{ for } j = 1, 2, 3. \quad (\text{A.6})$$

To prove (A.5) and (A.6) we appeal to lemma 1.20 of [24], and write

$$\mathcal{P}_\pm(\mu) = \tilde{\mathcal{P}}(\mu) + \mathcal{Q}_\pm(\mu), \quad (\text{A.7})$$

where

$$\tilde{\mathcal{P}}(\mu) = (\mu - \frac{1}{3}\alpha)^3 + \lambda,$$

$$\mathcal{Q}_+(\mu) = (\alpha^2 - c)\mu + \frac{1}{27}\alpha^3, \quad \mathcal{Q}_-(\mu) = (\alpha^2 + pc)\mu + \frac{1}{27}\alpha^3.$$

It then follows from this lemma that as $|\lambda| \rightarrow \infty$ with $\lambda \in \Omega_+$,

$$\mu^\pm = (-\lambda)^{1/3} + \frac{1}{3}\alpha + \mathcal{O}(|\lambda|^{-1/3}). \quad (\text{A.8})$$

It is straightforward to see that (A.8) implies that for $i = 0, 1$,

$$|(\mu_k^\pm)^j / \mathcal{P}'_\pm(\mu_j^\pm)| = o(1) \quad \text{for } j, k = 1, 2, 3,$$

as $|\lambda| \rightarrow \infty$ with $\lambda \in \Omega_+$. Therefore (A.3) and (A.4) are true for the KdV–Burgers equation. From (A.8), one may also show that

$$V^+ = V^- \cdot (I + o(1)), \quad (\text{A.9})$$

since $V_{jk}^\pm = (\mu_k^\pm)^{j-1}$. Combining (A.9) with (A.4) gives

$$\eta^-(0, \lambda) V^+ e_1 = 1 + o(1). \quad (\text{A.10})$$

Now to prove $D(\lambda) \rightarrow 1$ as $|\lambda| \rightarrow \infty$ with $\lambda \in \Omega_+$, we recall from (3.17) that

$$D(\lambda) = \eta^- \cdot \zeta^+ = \eta^- V^+ \cdot W^+ \zeta^+.$$

Then from (A.3) and (A.10) it is clear that $D(\lambda) = 1 + o(1)$. □

References

- [1] J. Alexander, R. Gardner and C.K.R.T. Jones, A topological invariant arising in the stability analysis of traveling waves, *Z. Reine Angew. Math.* 410 (1990) 167–212.
- [2] T.B. Benjamin, The stability of solitary waves, *Proc. R. Soc. London A* 328 (1972) 153–183.
- [3] D.J. Benney, Long waves on liquid films, *J. Math. Phys.* 45 (1966) 150–155.
- [4] J.L. Bona, On the stability of solitary waves, *Proc. R. Soc. London A* 344 (1975) 363–374.
- [5] J.L. Bona and M.E. Schonbek, Traveling wave solutions to the Korteweg–de Vries–Burgers equation, *Proc. R. Soc. Edin.* A 101 (1985) 207–226.
- [6] J.L. Bona, P.E. Souganidis and W.A. Strauss, Stability and instability of solitary waves, *Proc. R. Soc. London A* 411 (1987) 395–412.
- [7] J. Canosa and J. Gazdag, The Korteweg–de Vries–Burgers equation, *J. Comput. Phys.* 23 (1977) 393–403.
- [8] J.W. Evans, Nerve axon equations, IV: The stable and unstable impulse, *Indiana Univ. Math. J.* 24 (1975) 1169–1190.
- [9] J.W. Evans and J. Feroe, Local stability theory of the nerve impulse, *Math. Biosci.* 37 (1977) 23–50.
- [10] R. Gardner and C.K.R.T. Jones, Traveling waves of a perturbed diffusion equation arising in a phase field model, *Indiana Univ. Math. J.* 38 (1989) 1197–1222.
- [11] H. Grad and P.N. Hu, Unified shock profiles in a plasma, *Phys. Fluids* 10 (1967) 2596–2602.
- [12] D. Henry, *Geometric Theory of Semilinear Parabolic Equations*, Lecture Notes in Mathematics, Vol. 840 (Springer, New York, 1981).
- [13] P.N. Hu, Collisional theory of shock and nonlinear waves in a plasma, *Phys. Fluids* 15 (1972) 854–864.
- [14] R.S. Johnson, A nonlinear equation incorporating damping and dispersion, *J. Fluid Mech.* 42 (1970) 49–60.
- [15] R.S. Johnson, Shallow water waves on a viscous fluid – the undular bore, *Phys. Fluids* 15 (1972) 1693–1699.
- [16] C.K.R.T. Jones, Stability of the traveling wave solution to the FitzHugh–Nagumo equation, *Trans. Amer. Math. Soc.* 286 (1984) 431–469.
- [17] T. Kawahara, Weak nonlinear magneto-acoustic waves in a cold plasma in the presence of effective electron–ion collisions, *J. Phys. Soc. Japan* 27 (1970) 1321–1329.
- [18] M. Khodja, Nonlinear stability of oscillatory traveling waves for some systems of hyperbolic conservation laws. Ph.D. dissertation, University of Michigan (1989).
- [19] E.W. Laedke and K.H. Spatschek, Stability theorem for KdV type equations, *J. Plasma Phys.* 32 (1984) 263–272.
- [20] P. Lax, *Hyperbolic Systems of Conservation Laws and the Mathematical Theory of Shock Waves*, CBMS Lecture Notes, Vol. 11 (SIAM, Philadelphia, 1973).
- [21] J. Marsden and M. McCracken, *The Hopf Bifurcation and its Applications* (Springer, New York, 1976).
- [22] V.K. Melnikov, On the stability of the center for time periodic perturbations, *Trans. Moscow Math. Soc.* 12 (1964) 1–57.
- [23] R.L. Pego, Remarks on the stability of shock profiles for conservation laws with dissipation, *Trans. Amer. Math. Soc.* 291 (1985) 353–361.
- [24] R.L. Pego and M.I. Weinstein, Eigenvalues, and solitary wave instabilities, *Phil. Trans. R. Soc. London A* 340 (1992) 47–94.
- [25] R.L. Pego and M.I. Weinstein, Evans’ function, Melnikov’s integral and solitary wave instabilities, in: *Differential Equations with Applications to Mathematical Physics*, eds. W.F. Ames, E.M. Harrell II and J.V. Herod (Academic Press, San Diego, 1993).
- [26] G. Strang, On the construction and comparison of difference schemes, *SIAM J. Num. Anal.* 5 (1968) 506–517.
- [27] J. Swinton and J. Elgin, Stability of travelling pulse to a laser equation, *Phys. Lett. A* 145 (1990) 428–433.
- [28] D. Terman, Stability of planar wave solutions to a combustion model, *SIAM J. Math. Anal.* 21 (1990) 1139–1171.
- [29] M.I. Weinstein, On the solitary traveling wave of the generalized Korteweg–de Vries equation, in: *Nonlinear Systems of Partial Differential Equations in Applied Mathematics*, eds. B. Nicolaenko, D. Holm and J. Hyman, Lectures in Applied Mathematics, Vol. 23 (Amer. Math. Soc., 1986).

- [30] M.I. Weinstein, Lyapunov stability of ground states of nonlinear dispersive evolution equations, *Commun. Pure Appl. Math.* 39 (1986) 51–68.
- [31] M.I. Weinstein, Existence and dynamic stability of solitary wave solutions of equations arising in long wave propagation. *Commun. PDE* 12 (1987) 1133–1173.
- [32] E. Yanagida, Stability of fast traveling pulse solutions of the Fitzhugh–Nagumo equations, *J. Math. Biol.* 22 (1985) 81–104.